Math. Appl. 15(2s)2026, 76–93

An Approach of Nonlinear Energies over EEG Rhythms for Epileptic Seizure Detection

Amel Benzaid[1], Rafik Djemili[2*], Mohammed Salem[3] and Lamia Benzaid[4]

Abstract: *Detecting epileptic seizures from electroencephalographic (EEG) recordings remains a central task in the diagnosis of epilepsy and in the localisation of the epileptogenic zone. In this work we study how well nonlinear energy measures, evaluated separately on each EEG rhythm, can discriminate between seizure and non-seizure activity. Every EEG segment is split into its delta, theta, alpha, beta and gamma components by three alternative tools, namely a bank of Butterworth (IIR) band-pass filters, the discrete wavelet transform (DWT) and wavelet packet decomposition (WPD). On each component we compute five quantities (exponential energy, Teager energy, log energy, log-energy entropy and an energy derived from the bottleneck of an autoencoder), and the resulting 25 values form the input of three classifiers: a multilayer perceptron (MLP), a support vector machine (SVM) and a long short-term memory (LSTM) network. Perfect accuracy (100%) is reached on the Bonn recordings for both the normal/ictal and the interictal/ictal problems, while 99.9% and 100% are obtained on the Single Electrode and Bern-Barcelona collections. These figures are at least as good as those of several recently published approaches.*

Received: 05/08/2026 Accepted: 25/10/2026 Published: 17/11/2026

Introduction

Epilepsy is among the most common long-term neurological conditions; it manifests itself through repeated seizures, and nearly one patient in three keeps having them in spite of sustained drug therapy [39]. Because the EEG mirrors the electrical behaviour of cortical neurons, it is the reference examination for spotting seizure episodes [4, 7]. Reviewing long recordings by eye, however, demands an experienced neurophysiologist, is hampered by artefacts of external origin [52], and is made harder by the fact that ictal and seizure-free traces frequently look alike. Reliable automatic detectors would therefore relieve clinicians and improve the follow-up of patients whose seizures strike without warning.

[1,2]LRES Lab., Université 20 Août 1955-Skikda, Algeria.
[3]Department of Electrical and Electronic Engineering, Sabahattin Zaim University, Istanbul, Turkey.
[4]Department of Mechanical Engineering, Université 20 Août 1955-Skikda, Algeria.
Email: am.benzaid@univ-skikda.dz (ORCID 0009-0003-2929-1411),
r.djemili@univ-skikda.dz (ORCID 0000-0003-3476-567X),
mohammed.salem@izi.edu.tr (ORCID 0000-0002-2913-7671),
l.benzaid@univ-skikda.dz (ORCID 0009-0000-2933-6120).
[*]**Corresponding author:** Amel Benzaid.
2010 *Mathematics Subject Classification*: 92C55, 94A12, 68T05, 62H30.

Keywords: Electroencephalography (EEG), epileptic seizure detection, nonlinear energy, Teager energy, wavelet packet decomposition, discrete wavelet transform, neural networks.

A typical automatic pipeline chains signal conditioning, the computation of descriptors in the time, frequency or joint time-frequency domain, an optional selection step and a final decision stage. Among the solutions proposed so far are rule-based predictors [1], combinations of empirical mode decomposition (EMD) with autoregressive coefficients [67] and several wavelet-based schemes [13, 42]; surveys of the field, on the other hand, point to weak reproducibility and insufficient statistical validation [9, 54]. Nonlinear descriptors have been shown to reveal fine differences between focal and non-focal recordings [3], and EMD, DWT or WPD decompositions associated with learning machines report excellent scores [6], even though doubts remain about how well they generalise. Computing the descriptors band by band also makes it possible to see what each rhythm contributes to the decision [71].

Richer nonlinear tools can extract more of the information hidden in EEG data and thus make the analysis more dependable. Since the EEG rhythms are closely tied to the physiology of the brain, we focus here on energies evaluated on each rhythm: the exponential energy, the log energy, the log-energy entropy, the Teager energy and the code produced by the hidden layer of an autoencoder, which we interpret as an energy-like quantity. The overall workflow is sketched in Fig. 4: the energies are measured on the sub-bands and passed to three classifiers, namely an SVM, an MLP and an LSTM network. Our main contributions are listed below:

- A descriptor that gathers several nonlinear energies computed on the five EEG rhythms, obtained either with Butterworth (IIR) filters, with the DWT or with the WPD; as far as we are aware, such a descriptor has not been reported before.
- An analysis of the benefit of merging several nonlinear energies into one feature vector rather than using them in isolation.
- The construction of three feature vectors, one per decomposition technique, from the concatenated energies.
- An assessment of the approach with both classical machine-learning (ML) and deep-learning (DL) classifiers.

The remainder of the manuscript is arranged in the following way. Prior work on the topic is surveyed in the next section. The section on materials and methods introduces the three EEG collections, gives an overview of the pipeline, and details the decomposition tools, the energy descriptors, the classifiers and the performance indices. The results section reports and discusses the outcomes obtained for the different detection problems and positions them with respect to the literature; concluding remarks close the paper.

Related Work

As an indicator of signal strength, energy has frequently served to characterise EEG sub-bands, most often in conjunction with a wavelet decomposition [20, 21, 48, 49]. Wavelet methods are indeed predominant: an extreme learning machine fed with wavelet descriptors obtained 99.25% accuracy [75]; approximate and fuzzy approximate entropies taken from a five-level DWT were passed to MLP and SVM classifiers [37, 38]; energy,

entropy and standard deviation computed on a six-level WPD allowed an SVM to exceed 99% [66]; line length [24] and multiwavelet approximate entropy [25] were combined with neural networks; and good detection rates were likewise reported for DWT statistics reduced by PCA, ICA or LDA [64] and for DWT-based approximate entropy [47]. Deep architectures [27], encodings of time-frequency images [40] and temporal spiking neural networks [29] are among the more recent directions.

Descriptors built on energy have been studied far less. Kocadagli and Langari [35] sought EEG classifiers of low complexity, while Fasil and Rajesh [19] proposed an exponential energy computed in the time domain, which achieved 89% on the Bern-Barcelona data and 99.5% on the Bonn data. The Teager operator has served to quantify the energy of electrocorticograms and to follow the spread of seizures [76]; it was ranked among the most useful seizure descriptors [18] and, together with curve length and mean energy, it has fed an SVM detector [22]. These observations led us to examine several nonlinear energies jointly over the EEG rhythms.

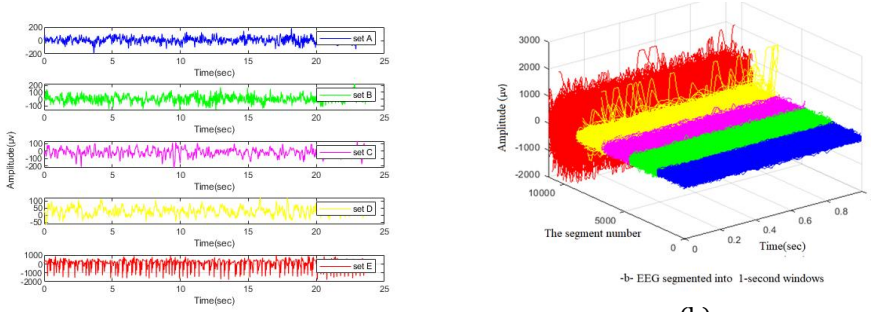
Materials and Methods

A. EEG Datasets

All experiments rely on three open EEG collections, so that the results can be reproduced and compared with previous studies.

1) Bonn University epileptic EEG database

The first collection is the Bonn database [14]. It is organised in five sets, A to E, of 100 single-channel segments lasting 23.6 s each. Sets A and B were taken from the scalp of five healthy, awake volunteers, with eyes open (A) or closed (B). Set C was recorded in the hippocampal formation of the hemisphere opposite to the epileptogenic zone and set D inside that zone, both during seizure-free periods, whereas set E contains only ictal activity. A single 128-channel acquisition system with common average referencing was used for every recording (Fig. 1); the data were sampled at 173.61 Hz with 12-bit precision and band-limited to 0.53–40 Hz (12 dB/octave). The files can be downloaded from [70].



(a) (b)

Fig. 1. Examples from the Bonn database: (a) one signal of each set A–E; (b) signals cut into 1 s windows.

2) Bern-Barcelona EEG database

The second collection was released in 2012 by the neurology department of the University of Bern. It gathers long-term intracranial recordings of five

epileptic patients, sampled at 512 Hz or 1024 Hz, whose channels were labelled as focal or non-focal by two experienced neurologists. Each signal covers 20 s, i.e. 10,240 samples. We used the Data_F_50.zip and Data_N_50.zip subsets (Fig. 2); a full description is given by Andrzejak et al. [8], and the files are distributed through [45, 69].

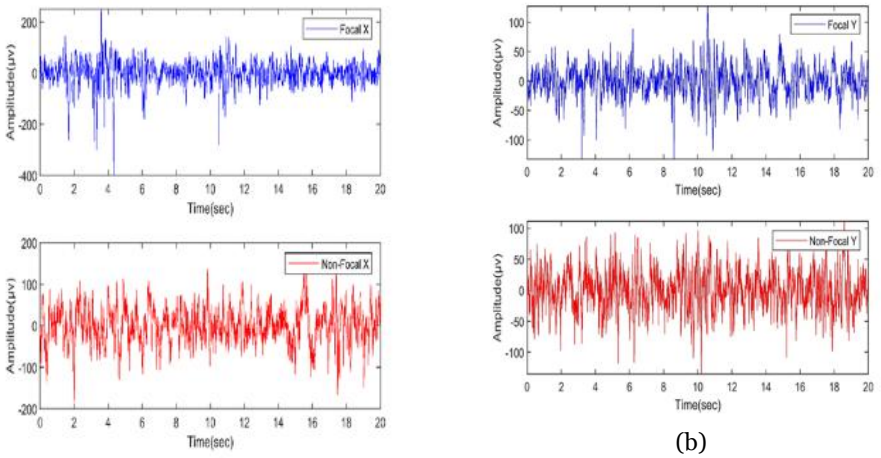


Fig. 2. Examples from the Bern-Barcelona database: (a) focal and non-focal channel X; (b) focal and non-focal channel Y.

3) Single Electrode EEG data of healthy and epileptic patients

The third collection, released in 2020, was assembled for building diagnostic models of epilepsy. Its sampling rate, filtering, number of signals and segment length follow those of the Bonn data, but, unlike the latter, it does not mix intracranial and scalp recordings across groups [50]: every signal comes from surface electrodes placed on 15 healthy or epileptic subjects (Fig. 3). It is available online at [60].

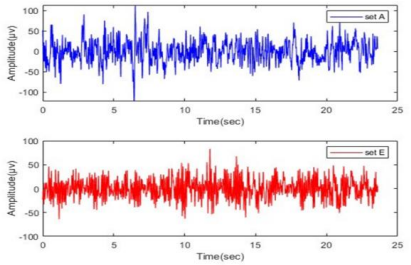


Fig. 3. Examples from the Single Electrode database.

B. Proposed Method

An EEG trace can be viewed as the superposition of five rhythms, delta (δ), theta (θ), alpha (α), beta (β) and gamma (γ), whose usual ranges are recalled in Table 1; since seizures alter these rhythms, they are a natural source of discriminative information. The processing chain of Fig. 4 first cuts the recording into segments and then separates each segment into the five rhythms by one of three tools: (1) Butterworth IIR band-pass filters, (2) the WPD or (3) the DWT. The nonlinear energies of every rhythm are finally computed and used to train and test the classifiers.

TABLE 1. Usual frequency ranges and amplitudes of the EEG rhythms [2].

Rhythm	Frequency (Hz)	Amplitude (µV)
Delta (δ)	0–4	20–100
Theta (θ)	4–8	10
Alpha (α)	8–12	2–100
Beta (β)	12–22	5–10
Gamma (γ)	>30	–

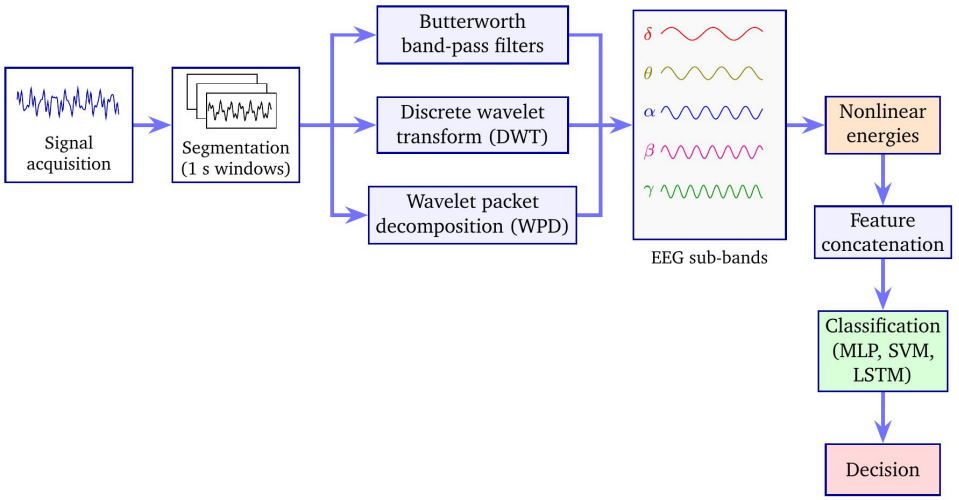


Fig. 4. Overview of the proposed detection scheme.

C. Sub-band Decomposition

1) Temporal filtering

A Butterworth filter belongs to the family of recursive (IIR) filters: each output sample is a linear combination of present and previous inputs and of previous outputs,

$$y(m) = \sum_{k=1}^{N} a_k \, y(m-k) + \sum_{k=0}^{M} b_k \, x(m-k) \qquad (1)$$

and its squared gain has no ripple and is as flat as possible in the passband [34]:

$$|H(j\omega)|^2 = \frac{1}{1+\left(\frac{\omega}{\omega_c}\right)^{2N}} \qquad (2)$$

Here N stands for the order and ω_c for the cutoff frequency. This monotonic gain makes the filter attractive for EEG work [53, 77]. We use five band-pass Butterworth filters of order five, a value retained after preliminary trials as a compromise between selectivity and cost, to isolate the five rhythms.

2) Wavelet Packet Decomposition (WPD)

Whereas the DWT only splits the approximation branch, the WPD splits the approximation and the detail branches alike at every level, which refines the frequency resolution at high frequencies [6]. With the db4 Daubechies wavelet adopted in this work, the wavelet packet functions read

$$W_{j,k}^{n}(t) = 2^{j/2} \, W^{n} \quad (2^{j}t - k) \qquad (3)$$

The scaling function and the mother wavelet correspond to $W^0 = \phi$ and $W^1 = \psi$, and the remaining functions are generated recursively:

$$W_{0,0}^{2n}(t) = \sqrt{2} \sum_{k} \; h\,(k) \, W_{1,k}^{n}(2t - k) \qquad (4)$$

$$W_{0,0}^{2n+1}(t) = \sqrt{2}\sum_k \; g(k)\, W_{1,k}^{n}(2t-k) \tag{5}$$

In these relations h and g denote the quadrature mirror filters linked to ϕ and ψ. Projecting a function f onto the packets gives the coefficients

$$W_{j,n,k} = \langle f,\, W_{j,k}^{n} \rangle = \int f(t)\, W_{j,k}^{n}(t)\, dt \tag{6}$$

Filtering both branches repeatedly with the low-pass and high-pass filters produces the complete packet tree; once its nodes are sorted by increasing frequency (Paley order) [72], it offers a flexible time-frequency description suited to stationary as well as non-stationary behaviour [74].

The rhythms used here, delta (0–5.5 Hz), theta (5.5–8 Hz), alpha (8–11 Hz), beta (11–22 Hz) and gamma (22–44 Hz), correspond to the shaded nodes of the tree in Fig. 5.

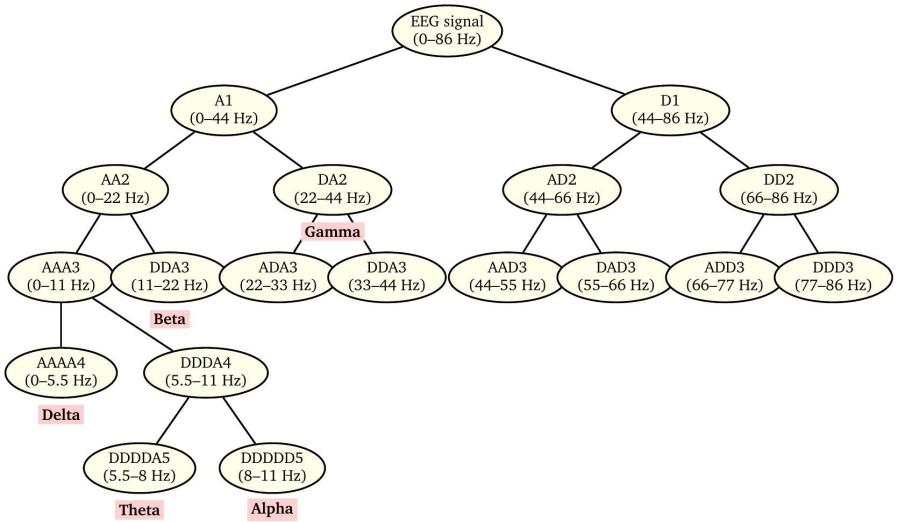


Fig. 5. Five-level wavelet packet tree; shaded nodes give the EEG rhythms.

3) Discrete Wavelet Transform (DWT)

For the DWT branch, the signal is decomposed over several levels with the db4 wavelet according to the tree of Fig. 6. This yields the details D1 (44–86 Hz), D2 (22–44 Hz), D3 (11–22 Hz), D4 (5.5–11 Hz) and D5 (2.75–5.5 Hz), together with the approximation A5 (0–2.75 Hz). Splitting A1 once more separates the alpha+beta content (0–22 Hz) from the gamma content (22–44 Hz). D4 is associated with theta and A4 with delta; D5 and A5 hold the slowest delta components, and D1 the fastest components of the signal.

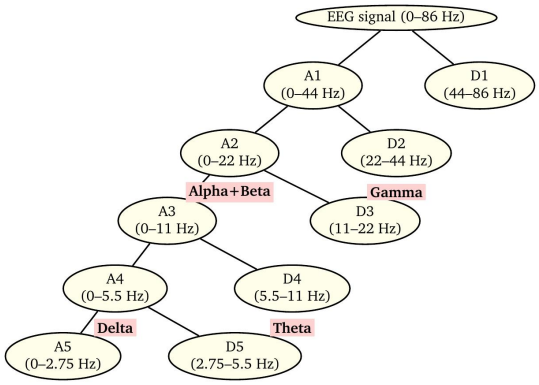


Fig. 6. DWT decomposition tree used to extract the EEG rhythms.

D. Nonlinear Energy Features

Five descriptors of an energetic nature are evaluated on every sub-band; in all cases, energy is understood as the area under the instantaneous power of the signal [49].

1) Exponential energy

Energy is a classical way of quantifying how strong a signal is [19]. In continuous time, the energy of $x(t)$ is the integral of its squared modulus:

$$E = \int_{-\infty}^{+\infty} |x(t)|^2 \, dt \tag{7}$$

and, for N samples in discrete time,

$$E = \sum_{n=1}^{N} |x(n)|^2 \tag{8}$$

Epileptic activity typically shows sharper and taller peaks, which inflates the quantities in (7)–(8) [19]. Exponential peak functions are a common way of flagging such irregular events [5, 23]; in line with [19], we use an exponential energy that gives less weight to large amplitudes:

$$ExpEn = \sum_{n=1}^{N} e^{\frac{x(n)^2}{\sigma}} \tag{9}$$

The parameter σ sets the width of the kernel. With σ = 1, any amplitude lying in [−2.15, 2.15] contributes at least 0.01 to the sum [19].

2) Teager energy (TE)

Ictal discharges are abrupt events of large amplitude and high frequency, and the Teager energy (TE) is particularly good at separating them from the ongoing background [30]. For a narrow-band signal with amplitude A and normalised angular frequency $\Omega = 2\pi f / f_s$ it equals

$$E_T = A^2 \sin^2(\Omega) \tag{10}$$

The corresponding Teager energy operator (TEO) takes the following forms in continuous and in discrete time [19]:

$$\psi[y(t)] = \dot{y}^2(t) - y(t)\,\ddot{y}(t) \tag{11}$$

$$\psi[y(n)] = y^2(n) - y(n-1)\,y(n+1) \tag{12}$$

Three neighbouring samples are enough to evaluate the discrete operator, which explains its fast response to transients. Slow oscillations are then discarded by thresholding the curve length of the TE sequence $y(n)$ computed over N consecutive values [19]:

$$\varphi[y(n)] = \sum_{k=n}^{n+N} |y(k-1) - y(k)| \tag{13}$$

3) Log-energy entropy

Entropy measures how complex or irregular a signal is [57], and its log-energy variant, associated with neural networks, has already been used to tell epileptic EEG apart from normal EEG [10]. It is obtained from the squared samples without any normalisation [55] and is written [26]

$$E_{SumLgEn} = \sum_{i=1}^{N} \log\left(x_i^2\right) \tag{14}$$

with x_i the i-th of the N samples.

4) Log energy

Taking the logarithm of the energy narrows its dynamic range and lessens the weight of very large values and of artefacts; small energy changes linked to seizures are thus easier to detect, at almost no extra cost [33, 41]:

$$E_{LgEn} = \log\left(\sum_{i=1}^{N} x_i^2\right) \tag{15}$$

again with x_i the i-th of the N samples.

5) Autoencoder (AE)

An autoencoder is a network built around a narrow central layer: its encoder compresses the input into a short latent code, from which its decoder tries to rebuild the input [12]. Encoding is expressed as

$$E_{AE} = f(\theta, x) = L(Wx + n) \tag{16}$$

in which $\theta = \{W, n\}$ gathers the weights and biases and L is the activation. The decoder then produces [28]

$$y = g(\theta', E_{AE}) = L(W'E_{AE} + n') \tag{17}$$

where $\theta' = \{W', n'\}$, so that the complete mapping reads

$$y = g_{\theta'}\left(f_\theta(x)\right) \tag{18}$$

Training adjusts the parameters by backpropagation so as to minimise the mean squared reconstruction error between x and y. The recordings are cut into consecutive, non-overlapping 1 s windows, and the code E_{AE} obtained for each window (Fig. 7) is taken as an additional energy-type descriptor.

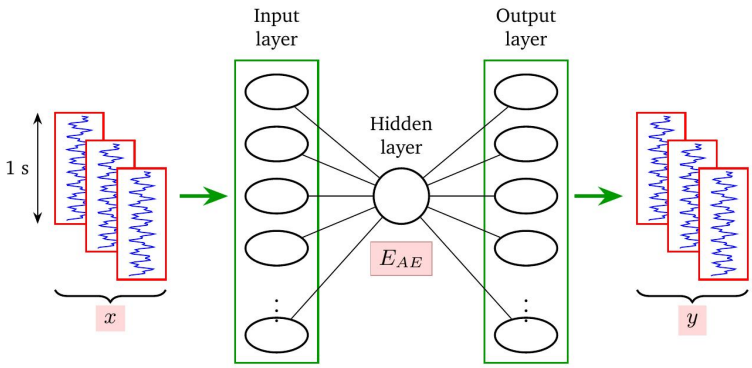


Fig. 7. Autoencoder used in this work: input x, latent code E_{AE} (hidden layer) and reconstruction y.

E. Classification Algorithms

We cast seizure detection as a two-class supervised problem: a model learnt from labelled examples assigns each new feature vector to one of the classes [56]. Three popular classifiers are compared.

1) Multilayer perceptron neural network (MLPNN)

The MLP is a feed-forward network made of an input layer, one or several hidden layers and an output layer; the size of the hidden layer controls the balance between under- and over-fitting. Its topology and settings were chosen with the procedure described by Djemili [16].

2) Support Vector Machines (SVM)

The SVM projects the data into a higher-dimensional space by means of a kernel and looks there for the separating hyperplane with the widest margin, which is fixed by a small set of support vectors. The training problem has a unique optimum, although its cost increases with the size of the training set [15].

3) Long Short-Term Memory (LSTM)

The LSTM is a recurrent architecture in which a memory cell, regulated by

input, forget and output gates, avoids the vanishing and exploding gradients met in plain recurrent networks. We use the configuration of Benzaid et al. [11].

F. Classifier Performance Evaluation

Three standard indices are reported to measure how well a two-class problem is solved: sensitivity (SE), specificity (SP) and classification accuracy (CA), given by

$$SE(\%) = \frac{NCP}{TNCP} \times 100 \tag{19}$$

Here NCP counts the positive (seizure) patterns that are recognised correctly and $TNCP$ is the number of positive patterns.

$$SP(\%) = \frac{NCN}{TNCN} \times 100 \tag{20}$$

Likewise, NCN is the number of negative (normal or interictal) patterns classified correctly and $TNCN$ the number of negative patterns; SE and SP are therefore the rates of correct "diseased" and "healthy" decisions.

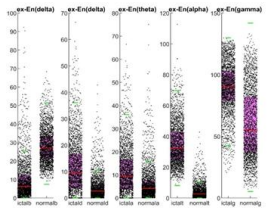
$$CA(\%) = \frac{NCC}{TNP} \times 100 \tag{21}$$

Finally, NCC is the number of correct decisions and TNP the total number of patterns.

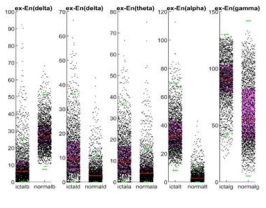
Results and Discussion

A. Feature Analysis

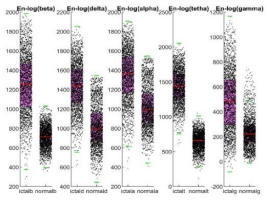
We now turn to the experimental findings. Following the scheme of Fig. 4, five nonlinear descriptors were measured on the delta (0–4 Hz), theta (4–8 Hz), alpha (8–13 Hz), beta (13–30 Hz) and gamma (>30 Hz) rhythms, each rhythm being isolated beforehand and its energies passed to the classifiers. Fig. 8 displays the distributions of the five descriptors (exponential energy, log-energy entropy, log energy, Teager energy and autoencoder code) for every rhythm. Ictal and normal segments, i.e. epileptic and healthy subjects, have clearly different average levels, which reflects the more regular and less random nature of normal EEG; this gap confirms that the descriptors are statistically meaningful. The scatter plots of Fig. 9, in which selected descriptors are plotted two by two for every rhythm, further show how the two classes occupy distinct regions of the feature plane.



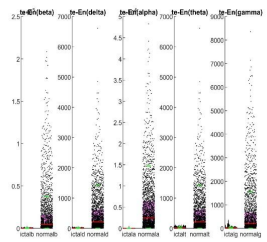
(a)



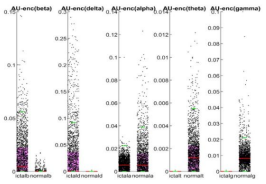
(b)



(c)

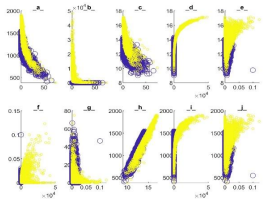


(d)

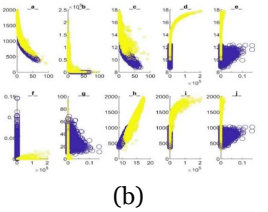


(e)

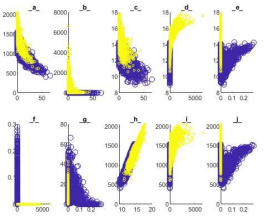
Fig. 8. Distribution (mean and SD) of the descriptors for ictal and normal EEG on the five rhythms: (a) exponential energy, (b) log-energy entropy, (c) log energy, (d) Teager energy, (e) autoencoder code.



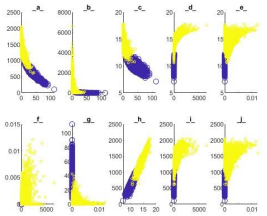
(a)



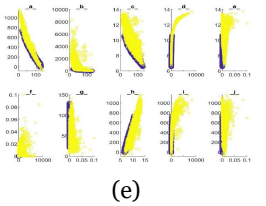
(b)



(c)



(d)



(e)

Fig. 9. Pairwise scatter plots of selected descriptors for the two classes after sub-band filtering: (a) alpha, (b) beta, (c) delta, (d) theta, (e) gamma.

B. Classification Results

Whatever the decomposition used (Butterworth filters, WPD or DWT), the five energies (exponential, Teager, logarithmic, log-energy entropy and autoencoder code) are computed on each of the five rhythms and stacked into a 25-component vector. The first classifier is a three-layer feed-forward network with 20 hidden and 2 output neurons, as in [16]; it uses a hyperbolic-tangent sigmoid in the hidden layer, a linear output and Levenberg–Marquardt training. The second is an SVM for which linear and polynomial kernels were tried, the polynomial one giving the best results. The third is a single-layer LSTM with 100 hidden units, trained with the ADAM optimiser for at most 70 epochs with mini-batches of 27 examples.

Each test amounts to deciding whether a segment is ictal or not, the non-ictal class gathering either healthy recordings or seizure-free periods of patients. On the Bonn data, six problems were considered: A–E, B–E, C–E, D–E, AB–E and CD–E, i.e. ictal set E against seizure-free segments of healthy volunteers (A, B) or of patients (C, D). The mean accuracies obtained by every classifier for every problem are listed in Table 2 and plotted in Fig. 10, while Table 3 gives the sensitivity and specificity of the MLP.

TABLE 2. Accuracy (%) obtained on the Bonn data with each decomposition method.

Case problem	Butterworth			WPD			DWT		
	MLP	**SVM**	**LSTM**	**MLP**	**SVM**	**LSTM**	**MLP**	**SVM**	**LSTM**
A–E	99.6	99.8	95.6	99.9	**100**	99.0	99.8	99.9	99.8
B–E	99.5	99.5	94.5	**100**	**100**	99.5	97.3	99.7	89.0
C–E	99.5	79.6	96.2	**100**	99.9	98.8	98.7	99.8	92.5
D–E	99.5	97.6	94.4	**99.9**	**99.9**	99.3	99.3	99.7	94.7
AB–E	94.5	93.0	92.9	99.9	**100**	**100**	99.6	99.0	96.8
CD–E	98.0	98.2	94.7	**99.8**	99.0	93.9	98.7	97.9	90.1

TABLE 3. Sensitivity (SE, %) and specificity (SP, %) of the MLP on the Bonn data.

Case problem	Butterworth		WPD		DWT	
	SE	**SP**	**SE**	**SP**	**SE**	**SP**
A–E	100	99.80	100	99.67	99.80	100
B–E	100	98.68	100	99.34	97.30	98.31
C–E	100	99.34	100	99.67	98.70	98.68
D–E	100	99.67	100	99.34	98.36	100
AB–E	100	99.01	100	99.67	99.83	96.76
CD–E	69.85	100	100	99.67	99.83	99.34

The same protocol was then repeated on the two other collections: healthy versus epileptic signals (A–E type) for the Single Electrode data, and focal versus non-focal signals, for both channels X and Y, for the Bern-Barcelona data (Table 4). As the bar chart of Fig. 11 shows for the four data sets, the MLP and the SVM perform best with Butterworth filtering and with the WPD, up to 100%. Butterworth filtering followed by an MLP thus appears as a particularly effective combination across the various detection problems.

TABLE 4. Accuracy (%) on the Single Electrode and Bern-Barcelona data.

Case problem	Butterworth			WPD			DWT		
	MLP	**SVM**	**LSTM**	**MLP**	**SVM**	**LSTM**	**MLP**	**SVM**	**LSTM**
Single Electrode	99.7	**99.9**	98.8	**99.9**	**99.9**	70.0	69.7	75.5	70.0
Bern-Barcelona X	**100**	**100**	89.5	99.5	**100**	99.5	**100**	81.5	99.5
Bern-Barcelona Y	99.7	89.0	99.6	99.9	99.5	99.5	**100**	78.5	99.5

The A–E problem is the easiest one, because sets A and E differ strongly; almost any descriptor or classifier separates them. At the other end, the C–E problem gives the weakest Bonn result, 79.60% for the SVM after Butterworth filtering, which can be explained by the resemblance between sets C and E. A comparable drop (69.7%, DWT with MLP) occurs on the Single Electrode data and is probably caused by the limited frequency resolution of the corresponding sub-bands.

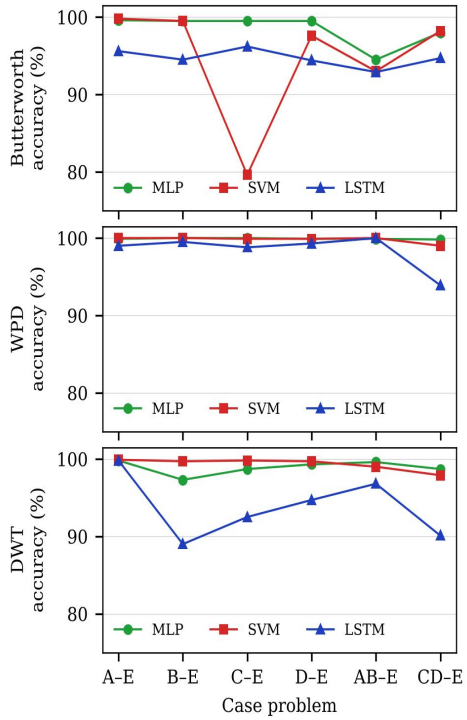


Fig. 10. Mean accuracy (%) for problems A–E, B–E, C–E, D–E, AB–E and CD–E with Butterworth, WPD and DWT decompositions.

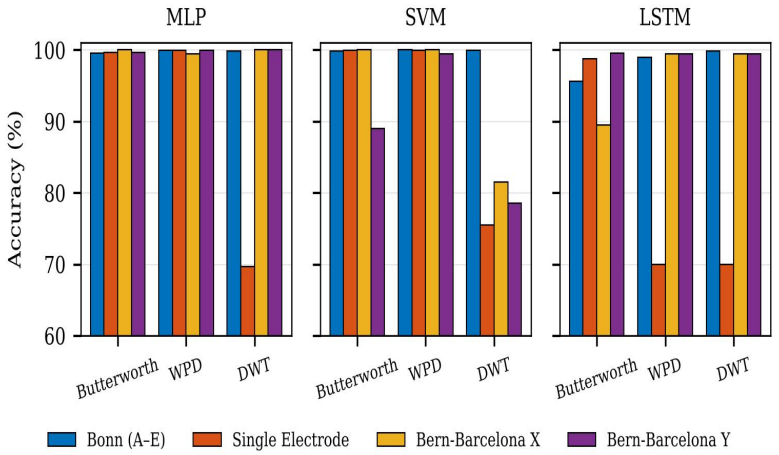


Fig. 11. Accuracy of the MLP, SVM and LSTM classifiers on the four data sets.

C. Comparison with Reported Studies

Table 5 sets our best accuracies against those reported by other seizure detection studies. Even though 100% is not achieved in every configuration, the proposed approach matches or outperforms a good part of the existing methods.

TABLE 5. Accuracies reported by other seizure detection studies.

Authors	Method	Database	Case	Accuracy (%)
Nigam et al. [44]	Neural network	Bonn	A–E	97.2
Srinivasan et al. [62]	ANN, time- and frequency-domain features	Bonn	A–E	99.6
Kannathal et al. [32]	Entropy measures	Bonn	A–E	92.22
Kannathal et al. [31]	Comparative study of nonlinear measures	Bonn	A–E	90
Polat et al. [51]	FFT + decision tree	Bonn	A–E	98.72
Subasi [63]	Wavelet features + mixture of experts	Bonn	A–E	95
Xiang et al. [73]	Fuzzy entropy	CHB-MIT	–	98.31
Kumar et al. [36]	Entropies + ANN	Bonn-Barcelona	–	94.5
Song et al. [61]	Optimized sample entropy + ELM	Bonn-Barcelona	–	99
Ocak [46]	Wavelet analysis + genetic algorithm	Private clinical data	–	94.3
Kannathal et al. [32]	Entropy measures	Bonn-Barcelona	–	90
Nicolaou et al. [43]	Permutation entropy + SVM	Bonn-Barcelona	–	94.38
Sharanreddy et al. [58]	Improved approximate entropy	CHB-MIT, Bonn	–	100
Shen et al. [59]	Physiology-based multichannel system	Private clinical data	–	91.18
Xiang et al. [73]	Fuzzy entropy	Bonn	–	100
Tzallas et al. [68]	Time-frequency analysis	Bonn	A–E	100
Benzaid et al. [11]	Nonlinear measures + deep learning	Bonn, Hauz Khas	A–E	100
Djemili et al. [17]	Nonlinear and chaos features, EMD/VMD	Bonn	A–E	100
Supriya et al. [65]	Complex network features	Bonn, Bern-Barcelona	–	99
Acharya et al. [3]	Focal EEG characterization (review)	Bern-Barcelona	–	85.89
This work	**Nonlinear energies over EEG rhythms + MLP/SVM/LSTM**	**Bonn; Single Electrode; Bern-Barcelona**	**A–E**	**100; 99.9; 100**

CONCLUSION

We have presented a seizure detection scheme that couples a rhythm-wise decomposition of the EEG with nonlinear energy descriptors: exponential energy, log energy, log-energy entropy, Teager energy and an autoencoder code. The rhythms were isolated with Butterworth filters, the WPD or the DWT, and the descriptors were classified with an MLP, an SVM and an LSTM network in order to recognise EEG patterns of healthy and epileptic subjects. The decomposition stage proved to be the key ingredient, providing compact and easily visualised representations without penalising the final decision, and the experiments showed that the scheme handles a wide range of classification problems. Butterworth filtering, in particular, conveys the influence of each rhythm on the energies and leads to very high detection rates. Future work will validate the approach on larger collections, extend it to other neurological disorders such as Alzheimer's disease and dementia, and apply it to other biosignals such as the ECG and the EMG.

Declarations

Conflict of interest. The authors are not aware of any financial or personal relationship that could have influenced this work.

Funding. No specific funding was received for this study.

Data availability. All three EEG collections are openly accessible [60, 69, 70]; any other data can be obtained from the corresponding author upon reasonable request.

References

[1] A. Aarabi and B. He, A rule-based seizure prediction method for focal neocortical epilepsy, Clin. Neurophysiol. 123 (2012), no. 6, 1111–1122.

[2] K. A. Aboalayon, H. T. Ocbagabir, and M. Faezipour, *Efficient sleep stage classification based on EEG signals*, IEEE Long Island Systems, Applications and Technology (LISAT) Conference, IEEE, 2014, pp. 1–6.

[3] U. R. Acharya, Y. Hagiwara, S. N. Deshpande, S. Suren, J. E. W. Koh, S. L. Oh, et al., *Characterization of focal EEG signals: a review*, Future Gener. Comput. Syst. **91** (2019), 290–299.

[4] U. R. Acharya, S. V. Sree, G. Swapna, R. J. Martis, and J. S. Suri, *Automated EEG analysis of epilepsy: a review*, Knowl.-Based Syst. **45** (2013), 147–165.

[5] M. Ahmad and F. M. Salam, *Dynamic learning using exponential energy functions*, Proceedings of the International Joint Conference on Neural Networks (IJCNN), vol. 2, IEEE, 1992, pp. 121–126.

[6] E. Alickovic, J. Kevric, and A. Subasi, *Performance evaluation of empirical mode decomposition, discrete wavelet transform, and wavelet packed decomposition for automated epileptic seizure detection and prediction*, Biomed. Signal Process. Control **39** (2018), 94–102.

[7] H. U. Amin, M. Z. Yusoff, and R. F. Ahmad, *A novel approach based on wavelet analysis and arithmetic coding for automated detection and diagnosis of epileptic seizure in EEG signals using machine learning techniques*, Biomed. Signal Process. Control **56** (2020), 101707.

[8] R. G. Andrzejak, K. Schindler, and C. Rummel, *Nonrandomness, nonlinear dependence, and nonstationarity of electroencephalographic recordings from epilepsy patients*, Phys. Rev. E **86** (2012), no. 4, 046206.

[9] E. B. Assi, D. K. Nguyen, S. Rihana, and M. Sawan, *Towards accurate prediction of epileptic seizures: a review*, Biomed. Signal Process. Control **34** (2017), 144–157.

[10] S. Aydin, H. M. Saraoğlu, and S. Kara, *Log energy entropy-based EEG classification with multilayer neural networks in seizure*, Ann. Biomed. Eng. **37** (2009), no. 12, 2626–2630.

[11] A. Benzaid, R. Djemili, and K. Arbateni, *Seizure detection using nonlinear measures over EEG frequency bands and deep learning classifiers*, Comput. Methods Biomech. Biomed. Eng. **28** (2025), no. 13, 2032–2048.

[12] K. Berahmand, F. Daneshfar, E. S. Salehi, Y. Li, and Y. Xu, *Autoencoders and their applications in machine learning: a survey*, Artif. Intell. Rev. **57** (2024), no. 2, 28.

[13] P. Boonyakitanont, A. Lek-Uthai, K. Chomtho, and J. Songsiri, *A review of feature extraction and performance evaluation in epileptic seizure detection using EEG*, Biomed. Signal Process. Control **57** (2020), 101702.

[14] J. D. Bronzino and D. R. Peterson, *Principles of electroencephalography*, Biomedical Engineering Fundamentals, CRC Press, Boca Raton, FL, 2006, pp. 445–456.

[15] C. Cortes and V. Vapnik, *Support-vector networks*, Mach. Learn. **20** (1995), no. 3, 273–297.

[16] R. Djemili, *Analysis of statistical coefficients and autoregressive parameters over intrinsic mode functions (IMFs) for epileptic seizure detection*, Biomed. Eng. Biomed. Tech. **65** (2020), no. 6, 693–704.

[17] R. Djemili and I. Djemili, *Nonlinear and chaos features over EMD/VMD decomposition methods for ictal EEG signals detection*, Comput. Methods Biomech. Biomed. Eng. **27** (2024), no. 15, 2091–2110.

[18] R. Esteller, *Detection of seizure onset in epileptic patients from intracranial EEG signals*, Ph.D. thesis, Georgia Institute of Technology, Atlanta, GA, 2000.

[19] O. K. Fasil and R. Rajesh, *Time-domain exponential energy for epileptic EEG signal classification*, Neurosci. Lett. **694** (2019), 1–8.

[20] P. Fergus, D. Hignett, A. Hussain, D. Al-Jumeily, and K. Abdel-Aziz, *Automatic epileptic seizure detection using scalp EEG and advanced artificial intelligence techniques*, BioMed Res. Int. **2015** (2015), 986736.

[21] T. Gandhi, B. K. Panigrahi, and S. Anand, *A comparative study of wavelet families for EEG signal classification*, Neurocomputing **74** (2011), no. 17, 3051–3057.

[22] A. B. Gardner, A. M. Krieger, G. Vachtsevanos, and B. Litt, *One-class novelty detection for seizure analysis from intracranial EEG*, J. Mach. Learn. Res. **7** (2006), 1025–1044.

[23] A. Golubev, *Exponentially modified peak functions in biomedical sciences and related disciplines*, Comput. Math. Methods Med. **2017** (2017), 7925106.

[24] L. Guo, D. Rivero, J. Dorado, J. R. Rabuñal, and A. Pazos, *Automatic epileptic seizure detection in EEGs based on line length feature and artificial neural networks*, J. Neurosci. Methods **191** (2010), no. 1, 101–109.

[25] L. Guo, D. Rivero, and A. Pazos, *Epileptic seizure detection using multiwavelet transform based approximate entropy and artificial neural networks*, J. Neurosci. Methods **193** (2010), no. 1, 156–163.

[26] V. Gupta, T. Priya, A. K. Yadav, R. B. Pachori, and U. R. Acharya, *Automated detection of focal EEG signals using features extracted from flexible analytic wavelet transform*, Pattern Recognit. Lett. **94** (2017), 180–188.

[27] X. Huang, H. Meng, and Z. Li, *Deep learning for epileptic seizure prediction from EEG signals: a review*, Biomed. Signal Process. Control **117** (2026), 109518.

[28] J. F. Hwaidi and T. M. Chen, *Classification of motor imagery EEG signals based on deep autoencoder and convolutional neural network approach*, IEEE Access **10** (2022), 48071–48081.

[29] G. S. Jebaraj and K. Elango, *EEG seizure classification with temporal spiking neural networks and mutual information-based feature selection*, J. Eng. Appl. Sci. **72** (2025), no. 1, 218.

[30] C. Kamath, *ECG beat classification using features extracted from Teager energy functions in time and frequency domains*, IET Signal Process. **5** (2011), no. 6, 575–581.

[31] N. Kannathal, U. R. Acharya, C. M. Lim, and P. K. Sadasivan, *Characterization of EEG—a comparative study*, Comput. Methods Programs Biomed. **80** (2005), no. 1, 17–23.

[32] N. Kannathal, M. L. Choo, U. R. Acharya, and P. K. Sadasivan, *Entropies for detection of epilepsy in EEG*, Comput. Methods Programs Biomed. **80** (2005), no. 3, 187–194.

[33] S. A. Karthik, K. N. Bharath, B. R. Ramji, K. Puttegowda, B. Aruna, and D. S. Kumar, *Enhanced EEG signal processing for accurate epileptic seizure detection*, SN Comput. Sci. **6** (2025), no. 6, 608.

[34] A. M. Katiyar, *Design of Butterworth and Chebyshev1 lowpass filter for equalized group delay*, Int. J. **2** (2012), no. 5.

[35] O. Kocadagli and R. Langari, *Classification of EEG signals for epileptic seizures using hybrid artificial neural networks based wavelet transforms and fuzzy relations*, Expert Syst. Appl. **88** (2017), 419–434.

[36] S. P. Kumar, N. Sriraam, P. G. Benakop, and B. C. Jinaga, *Entropies based detection of epileptic seizures with artificial neural network classifiers*, Expert Syst. Appl. **37** (2010), no. 4, 3284–3291.

[37] Y. Kumar, M. L. Dewal, and R. S. Anand, *Epileptic seizure detection using DWT based fuzzy approximate entropy and support vector machine*, Neurocomputing **133** (2014), 271–279.

[38] ———, *Epileptic seizures detection in EEG using DWT-based ApEn and artificial neural network*, Signal Image Video Process. **8** (2014), no. 7, 1323–1334.

[39] P. Kwan and M. J. Brodie, *Early identification of refractory epilepsy*, N. Engl. J. Med. **342** (2000), no. 5, 314–319.

[40] J. W. Li, G. Y. Feng, J. J. Lv, et al., *A rhythmic encoding approach based on EEG time-frequency image for epileptic seizure detection*, Biomed. Signal Process. Control **99** (2025), 106824.

[41] W. Li, L. Wang, Y. Zhou, H. Bourlard, and Q. Liao, *Robust log-energy estimation and its dynamic change enhancement for in-car speech recognition*, IEEE Trans. Audio Speech Lang. Process. **21** (2013), no. 8, 1689–1698.

[42] Y. Liu, W. Zhou, Q. Yuan, and S. Chen, *Automatic seizure detection using wavelet transform and SVM in long-term intracranial EEG*, IEEE Trans. Neural Syst. Rehabil. Eng. **20** (2012), no. 6, 749–755.

[43] N. Nicolaou and J. Georgiou, *Detection of epileptic electroencephalogram based on permutation entropy and support vector machines*, Expert Syst. Appl. **39** (2012), no. 1, 202–209.

[44] V. P. Nigam and D. Graupe, *A neural-network-based detection of epilepsy*, Neurol. Res. **26** (2004), no. 1, 55–60.

[45] Nonlinear Time Series Analysis Group, Universitat Pompeu Fabra, *Nonrandomness, nonlinear dependence, and nonstationarity of electroencephalographic recordings from epilepsy patients (data set)*, https://www.upf.edu/web/ntsa/downloads, 2012.

[46] H. Ocak, *Optimal classification of epileptic seizures in EEG using wavelet analysis and genetic algorithm*, Signal Process. **88** (2008), no. 7, 1858–1867.

[47] ———, *Automatic detection of epileptic seizures in EEG using discrete wavelet transform and approximate entropy*, Expert Syst. Appl. **36** (2009), no. 2, 2027–2036.

[48] I. Omerhodzic, S. Avdakovic, A. Nuhanovic, and K. Dizdarevic, *Energy distribution of EEG signals: EEG signal wavelet-neural network classifier*, World Acad. Sci. Eng. Technol. **37** (2013), 1240–1245.

[49] R. Panda, P. S. Khobragade, P. D. Jambhule, S. N. Jengthe, P. R. Pal, and T. K. Gandhi, *Classification of EEG signal using wavelet transform and support vector machine for epileptic seizure diction*, 2010 International Conference on Systems in Medicine and Biology, IEEE, 2010, pp. 405–408.

[50] S. Panwar, S. D. Joshi, A. Gupta, and P. Agarwal, *Automated epilepsy diagnosis using EEG with test set evaluation*, IEEE Trans. Neural Syst. Rehabil. Eng. **27** (2019), no. 6, 1106–1116.

[51] K. Polat and S. Güneş, *Classification of epileptiform EEG using a hybrid system based on decision tree classifier and fast Fourier transform*, Appl. Math. Comput. **187** (2007), no. 2, 1017–1026.

[52] S. C. Ponten, H. E. Ronner, R. L. M. Strijers, M. C. Visser, S. M. Peerdeman, W. P. Vandertop, et al., *Feasibility of online seizure detection with continuous EEG monitoring in the intensive care unit*, Seizure **19** (2010), no. 9, 580–586.

[53] R. Ramesh and S. A. Kumar, *Emergence of digital libraries and digitization in India: issues and challenges*, Emerging Technologies in Libraries: Trends and Developments, p. 245.

[54] B. Schelter, M. Winterhalder, T. Maiwald, A. Brandt, A. Schad, J. Timmer, and A. Schulze-Bonhage, *Do false predictions of seizures depend on the state of vigilance? A report from two seizure-prediction methods and proposed remedies*, Epilepsia **47** (2006), no. 12, 2058–2070.

[55] M. Selik, R. Baraniuk, and A. Blair, *Signal energy versus signal power*, OpenStax-CNX module m10055, http://cnx.rice.edu/content/m10055/2.4, 2001.

[56] J. Seo, T. H. Laine, and K.-A. Sohn, *Machine learning approaches for boredom classification using EEG*, J. Ambient Intell. Humaniz. Comput. **10** (2019), no. 10, 3831–3846.

[57] C. E. Shannon, *A mathematical theory of communication*, Bell System Tech. J. **27** (1948), 379–423.

[58] P. Sharanreddy and P. K. Kulkarni, *EEG signal classification for epilepsy seizure detection using improved approximate entropy*, Int. J. Public Health Sci. **2** (2013), no. 1, 23–32.

[59] C. P. Shen, S. T. Liu, W. Z. Zhou, F. S. Lin, A. Y. Y. Lam, H. Y. Sung, et al., *A physiology-based seizure detection system for multichannel EEG*, PLoS One **8** (2013), no. 6, e65862.

[60] *Single electrode EEG data of healthy and epileptic patients (data set)*, Zenodo, https://zenodo.org/record/3684992, 2020.

[61] Y. Song, J. Crowcroft, and J. Zhang, *Automatic epileptic seizure detection in EEGs based on optimized sample entropy and extreme learning machine*, J. Neurosci. Methods **210** (2012), no. 2, 132–146.

[62] V. Srinivasan, C. Eswaran, and N. Sriraam, *Artificial neural network based epileptic detection using time-domain and frequency-domain features*, J. Med. Syst. **29** (2005), no. 6, 647–660.

[63] A. Subasi, *EEG signal classification using wavelet feature extraction and a mixture of expert model*, Expert Syst. Appl. **32** (2007), no. 4, 1084–1093.

[64] A. Subasi and M. I. Gursoy, *EEG signal classification using PCA, ICA, LDA and support vector machines*, Expert Syst. Appl. **37** (2010), no. 12, 8659–8666.

[65] S. Supriya, S. Siuly, H. Wang, and Y. Zhang, *New feature extraction for automated detection of epileptic seizure using complex network framework*, Appl. Acoust. **180** (2021), 108098.

[66] P. Swami, A. K. Godiyal, J. Santhosh, B. K. Panigrahi, M. Bhatia, and S. Anand, *Robust expert system design for automated detection of epileptic seizures using SVM classifier*, 2014 International Conference on Parallel, Distributed and Grid Computing, IEEE, 2014, pp. 219–222.

[67] A. K. Tafreshi, A. M. Nasrabadi, and A. H. Omidvarnia, *Empirical mode decomposition in epileptic seizure prediction*, 2008 IEEE International Symposium on Signal Processing and Information Technology, IEEE, 2008, pp. 275–280.

[68] A. T. Tzallas, M. G. Tsipouras, and D. I. Fotiadis, *Epileptic seizure detection in EEGs using time–frequency analysis*, IEEE Trans. Inf. Technol. Biomed. **13** (2009), no. 5, 703–710.

[69] Universitat Pompeu Fabra, *The Bern–Barcelona EEG database*, UPF Digital Repository, https://repositori.upf.edu/handle/10230/42829.

[70] ———, *EEG time series database*, UPF Digital Repository, https://repositori.upf.edu/handle/10230/42894.

[71] R. Upadhyay, A. Manglick, D. K. Reddy, P. K. Padhy, and P. K. Kankar, *Channel optimization and nonlinear feature extraction for electroencephalogram signals classification*, Comput. Electr. Eng. **45** (2015), 222–234.

[72] M. V. Wickerhauser, *Adapted wavelet analysis from theory to software*, A K Peters, Wellesley, MA, 1994.

[73] J. Xiang, C. Li, H. Li, R. Cao, B. Wang, X. Han, and J. Chen, *The detection of epileptic seizure signals based on fuzzy entropy*, J. Neurosci. Methods **243** (2015), 18–25.

[74] G. G. Yen and K. C. Lin, *Wavelet packet feature extraction for vibration monitoring*, IEEE Trans. Ind. Electron. **47** (2000), no. 3, 650–667.

[75] Q. Yuan, W. Zhou, J. Zhang, S. Li, D. Cai, and Y. Zeng, *EEG classification approach based on the extreme learning machine and wavelet transform*, Clin. EEG Neurosci. **43** (2012), no. 2, 127–132.

[76] H. P. Zaveri, W. J. Williams, and J. C. Sackellares, *Energy based detection of seizures*, Proceedings of the 15th Annual International Conference of the IEEE Engineering in Medicine and Biology Society, IEEE, 1993, pp. 363–364.

[77] D. X. Zhang, X. P. Wu, and X. J. Guo, *The EEG signal preprocessing based on empirical mode decomposition*, 2008 2nd International Conference on Bioinformatics and Biomedical Engineering, IEEE, 2008, pp. 2131–2134.